2023

Development of a Screening Methodology for the Analysis of Rhodamine B in Foodstuffs

George T. Knecht
University of Central Florida

DEVELOPMENT OF A SCREENING METHODOLOGY FOR THE ANALYSIS OF RHODAMINE B IN FOODSTUFFS

by

GEORGE THOMAS KNECHT

A thesis submitted in partial fulfillment of the requirements
for the Honors in the Major Program in Chemistry
in the College of Sciences
and the Burnett Honors College
at the University of Central Florida
Orlando, Florida

Spring Term, 2023

Thesis Chair: Andres D. Campiglia, Ph.D.

ABSTRACT

Synthetic dyes that are used as color additives in foodstuffs are regulated by the Food and Drug Administration (FDA) under the Food, Drug, and Cosmetic Act (FD&C). The use of synthetic dyes not approved by the FDA, or the addition of dyes approved by the FDA above their maximum concentration limits in foodstuffs necessarily constitutes illegal food adulteration. Recently, rhodamine B (RhB), a bright-pink synthetic dye not approved for use in foodstuffs, has become an adulterant of interest due to its discovery in a large variety of food samples, and its identity as a potential carcinogen. Numerous chromatographic and spectroscopic methods have been developed for the analysis of RhB in food samples, as well as standard methods available for the analysis of synthetic dyes. However, due to the complexity of real food samples and the chemical diversity of synthetic dye concomitants, comprehensive chromatographic methods tend to be time consuming and expensive. Herein, we report a method for the determination of RhB in foodstuffs for the screening of real samples prior to subsequent full-blown chromatographic analysis, saving valuable time and resources. This screening method employs thin-layer chromatography (TLC) as a separation method, and, due to the strong yellow-orange fluorescence exhibited by RhB when excited with ultraviolet or green light, direct fluorescent measurement of RhB on the TLC plate using a fiber optic probe coupled to a commercial spectrofluorometer or to an instrumental set up for laser-induced fluorescence measurements. Qualitative analysis of RhB is based on its retardation factor, excitation and fluorescence spectra, and fluorescence lifetime. Quantitative measurements are made directly from the TLC plate to provide analytical figures of merit comparable to traditional fluorometric methods in liquid solution. The ability of the new method to determine RhB in food samples is then demonstrated with the analysis of chili powder.

ACKNOWLEDGEMENTS

The author would like to acknowledge Andres D. Campiglia for his excellent mentorship as a principal investigator, as well as group members Anthony Santana, Stephanie Nauth, and Noah Froelich for their support throughout this project.

TABLE OF CONTENTS

LIST OF TABLES

LIST OF FIGURES

1. INTRODUCTION

1.1. Theis Question

Can an inexpensive, rapid screening method for the determination of rhodamine B in foodstuffs based on thin-layer chromatography (TLC) be developed, avoiding the use of industry-standard, expensive, and time-consuming chromatographic methodology?

1.2. Background and Significance

Food adulteration is a serious problem facing many countries across the world today. In the United Sates, one criterion for a food to be considered adulterated is the presence of unsafe color additives.[1] These color additives are regulated by the Food and Drug Administration (FDA) through the Federal Food, Drug, and Cosmetic act (FD&C). Under the FD&C, only color additives found in a maintained list approved by the FDA are legal for use in foodstuffs,[1,2] essentially forming a whitelist of allowed compounds. Any color additive found in foodstuffs that is not also present on this list necessarily constitutes an illegal adulteration of said foodstuffs. Unfortunately, despite FDA regulations and many similar regulations across the world,[3] illegally added synthetic dyes have been shown to be present in several food products in many countries.[4–16] In addition to constituting illegal adulteration, these dyes are often known to be hazardous to human health due to their toxicity, carcinogenicity, and/or mutagenicity.[17]

Of the many hazardous color additives found in adulterated foodstuffs, significant attention has been drawn to the synthetic dye rhodamine B in recent years. Rhodamine B (Figure 1) has been found in many food products,[14,15] and as a potential carcinogen,[17] represents a serious hazard to human health. Currently, methods for the quantitative analysis of rhodamine B in foodstuffs are

largely limited to high-performance liquid chromatography (HPLC) and triple quadrupole tandem mass spectrometry (LC-MS/MS). While these methods have been shown to be powerful tools for the analysis of hazardous dyes in food products, they are not well suited for the routine analysis of numerous samples. Their assays are laborious and time consuming, taking up to hours for a single run. Pure standards must be run periodically to verify retention times, which lengthens overall analysis. If the concentrations of target dyes are found to lie outside the detector's response range, the sample must be diluted (or concentrated), and the process repeated. The overhead cost of instrumentation required for these methods (pumps, columns, detectors, etc.) is large. Additionally, running these assays requires large volumes of highly pure and expensive mobile phase, which requires costly disposal protocols after use, representing a high operating cost. Because of the limitations presented by HPLC and LC-MS/MS methodology, and the importance of the determination of hazardous rhodamine B dye in adulterated foodstuffs, it is of great interest to develop an inexpensive, rapid screening method for the routine analysis of potentially adulterated food samples.

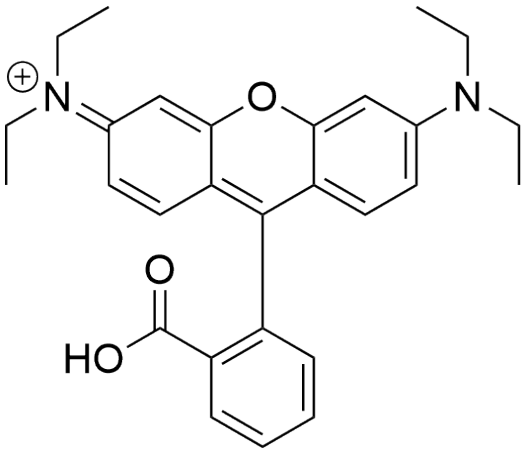

Figure 1: Chemical Structure of Rhodamine B

1.3. Thesis Goals

Shown here is a method based on TLC-SS-RTPLS (thin-layer chromatography solid-surface photoluminescence spectroscopy). An instrumental setup based on a fiber optic probe (FOP) coupled to one of two spectrofluorometers will be assembled, and confirmation of dye identity will be made directly on the TLC plate by recording excitation and emission spectra and photoluminescence lifetime. Since the probability of a concomitant with identical R_f (retardation factor) values having equivalent maximum excitation and emission wavelengths and photoluminescence lifetimes is almost inexistent, further HPLC separation is not necessary for confirmation using this method.

2. LITERATURE REVIEW

2.1. Summary of Synthetic Dyes in Adulterated Food Products

Analysis of synthetic dyes in adulterated food products has been a popular area of research in the past five years. These illegally added dyes span a large range of chromophore groups, have varied acidic or basic properties as well as spanning a wide range of polarities, and are found in varied and complex matrices. For these reasons, chromatographic methods have dominated the field. However, when performing traditional chromatography, different conditions are required for the different chromophore groups: triphenylmethane,[18,19] xanthene,[20,21] anthraquinone,[22,23] and azo dyes,[4,11] for example, all require varied mobile phases, flowrates, and/or gradients. Addition complexity is added by substituents, which can require pH and polarity adjustments within a given chromophore group.[5]

Adding additional complexity to the analysis of these dyes are the many varied matrices they are found in. Foodstuffs provide a wide variety of complex matrices that sometimes require different extraction and sample-prep procedures depending on their composition, which can include defatting of foods high in natural or added fats.[14] This also complicates extraction, as a given dye may be either fat soluble or fat insoluble, depending on polarity, and extraction methods will depend on the polarity of the medium and of the dye analyte.

Toxicity, carcinogenicity, and genotoxicity of illegal color additives in foodstuffs is of major concern. Toxicity values of dyes are given by their LD_{50} values — the dose measured to kill half the members of a tested population — and as either possibly or potentially carcinogenic, or possibly or potentially genotoxic. Almost all illegal color additives found in adulterated food products exhibit possible or potential carcinogenicity, and many are potentially genotoxic as

well.[17] A summary of the major illegal dyes that have been found in adulterated foodstuffs, including the matrices/products in which they were found, and their relevant toxicological information, is found in Table 1.

2.2. Standard Methods for the Analysis of Dyes in Food

Current standard methods for the analysis of food dyes in real samples are primarily focused on solid-phase extraction (SPE) followed by thin-layer chromatographic and spectrophotometric identification. Analysis is done visually by matching color, spectral features, and R_f values of unknown dyes within a food sample to reference standards.[24] This method provides only qualitative information, not quantitative data, and is only approved for use with certain FD&C color additives.[25] It has been suggested to automate this process by using a high-performance liquid chromatography photodiode array detection (HPLC-PDA) based method. This method has been shown to be successful in the identification of many color additives based on retention time and spectral profile and has successfully provided quantitative data based on chromatographic peak height.[26] However, this method is limited by the aforementioned expense of liquid chromatography and has not been widely adopted. Fluorescence has been used in standard methods to provide additional qualitative information to the identity of a dye through visual determination, considering the color of fluorescence,[27] but neither photoluminescent spectral information nor photoluminescent lifetimes have been implemented as qualitative or quantitative measures of color additive analysis.

2.3. Current Methods for the Analysis of Rhodamine B

When reviewing the literature for analysis of rhodamine B in food samples, it can be seen that there are two groups of methods currently published: full quantitative and semi-quantitative methods. Quantitative methods have been developed that use UV-Vis spectrophotometry,[28] liquid chromatography tandem mass spectrometry (LC-MS/MS),[29] HPLC-PDA,[30] traditional fluorescence spectroscopy, micelle-stabilized fluorescence spectroscopy (MS-RTF),[31] synchronous scan fluorescence spectroscopy,[32] and surface enhanced Raman spectroscopy on TLC plates (TLC-SERS).[33] Each of these methods has a major drawback that may make it undesirable for routine analysis of real food samples. The method using UV-Vis spectroscopy does not perform separation prior to analysis, which allows for the possibility of matrix interference in complex samples, as well as suffering from relatively high limits of detection (LODs) in the $\mu g\ mL^{-1}$ range. While fluorescence spectroscopy is more selective than absorption spectroscopy, traditional fluorescence spectroscopy and MS-RTF likewise do not incorporate separation to reduce the effect of concomitants, and while synchronous scan fluorescence spectroscopy can greatly reduce the effect of concomitants and spectral interference without chromatographic separation, this can be limited in highly-complex real samples such as foodstuffs,[34] especially with the presence of several spectrally similar dyes. The method using HPLC-PDA relies on expensive and time-consuming chromatographic methods as previously discussed, and the LC-MS/MS method has similar drawbacks, as well as an expensive and inaccessible detection method. Finally, while the TLC-SERS method provides inexpensive separation, it has a relatively high LOD similar to the UV-Vis method, around 1.0 ppm, which is above the average contamination value reported in literature, around 0.7 ppm.[35]

In addition to these methods, solid-substrate room-temperature photoluminescence spectroscopy (SS-RTPLS) has been used with a custom hydrogel solid-phase extraction membrane,[35] but results were limited to semi-quantitative analysis, and the synthesis of a custom hydrogel is required, limiting the scalability of this approach. Until now, TLC fluorescence analysis of rhodamine B in foodstuffs has been limited to either semi-quantitative visual analysis under UV lamps,[30] or the laborious scrape-dissolution method.[15] In this method, shown in Figure 2, a match in R_f and color provides evidence as to the identity of the component, where R_f is defined as the ratio between the distance traveled by the TLC spot (d_R) and the distance of the solvent front (d_M) on the TLC plate. To verify identity in the scrape-dissolution method, the TLC spot is scraped off the plate and the media extracted with solvent before centrifugation and subjection to further spectroscopic analysis. Quantitative analysis of the dye is performed by submitting a pure dye standard solution to the entire experimental procedure.

A summary of extraction procedures found in literature for the analysis of rhodamine B in foodstuffs is compiled in Table 2. A summary of TLC conditions is compiled in Table 3.

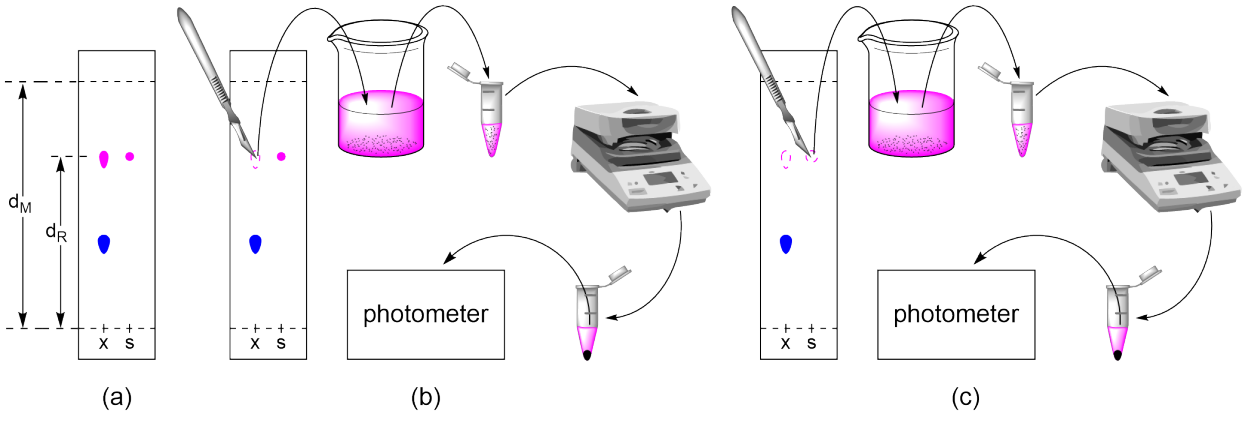

Figure 2: The scrape-dissolution analysis procedure

2.4. Solid-Substrate Room Temperature Photoluminescence Spectroscopy

SS-RTPLS is a technique that measures the emission of photoluminescence (fluorescence and/or phosphorescence) from compounds adsorbed on solid substrates.[36,37] Due to increased rigidity of the luminophore when adsorbed to the substrate, quantum efficiency of the luminophore is generally improved. This is able to provide improved LODs at trace mass levels (10^{-12} g – 10^{-9} g) and with sample volumes in the microliter range. Additionally, as a non-destructive method, solid substrates can be extracted for subsequent compound identification via high resolution techniques, after their initial SS-RTPLS analysis.

2.5. Multi-Dimensional and High-Order Data

In the field of chemometrics, the second-order advantage is well known.[38] This involves the improvement of analyte determinization when data spanning multiple variables are collected and analyzed. Spectroscopically, these data formats include excitation-emission matrices (EEMs), wavelength time matrices (WTMs) and time-resolved excitation-emission matrices (TREEMs).[39–41] Each of these data formats provides the second order advantage; combining multiple of these formats increases the order above two, improving the analysis further. When this higher-order instrumental data is processed with multi-way calibration algorithms, it is possible to identify and quantify targeted compounds regardless of how many signal-overlapping constituents the unknown sample contains.[41–45] In TLC analysis, this is extremely useful when compounds have identical R_f values as well as similar photoluminescent spectra, as they can be deconvoluted from one another and successfully analyzed using chemometric techniques, without the need for further separation.

Table 1: Dyes used in adulterated food products, products they are found in, and toxicities

Dye	Found in	Toxicity[17, a]	Refs
Rhodamine B	Sweets, bakery products, tamarind, saffron, chili powder, pepper, chili oil, pepper oil	LD_{50} (mouse) 887 mg kg^{-1} Potentially genotoxic Potentially carcinogenic	14–16
Sudan I	Ketchup, tomato sauce, chili powder, chili sauce, candy, sausage, turmeric powder, paprika, cumin, sumac, curry, saffron	LD_{50} (rabbit) <500 mg kg^{-1} Dermal sensitizer Genotoxic Potentially carcinogenic	7–12
Sudan II	Ketchup, tomato sauce, chili powder, chili sauce, candy, sausage, turmeric powder, paprika, cumin, sumac, curry	Genotoxic Possibly carcinogenic	7–11
Sudan III	Ketchup, tomato sauce, chili powder, chili sauce, candy, sausage, turmeric powder, paprika, cumin, sumac, curry, saffron	Possibly genotoxic Possibly carcinogenic	7–12
Sudan IV	Ketchup, tomato sauce, chili powder, chili sauce, candy, sausage, turmeric powder, paprika, cumin, sumac, curry	Potentially genotoxic Possibly carcinogenic	7–11
Sudan Red G	Chili powder, sausage, saffron, chili sauce, turmeric	Potentially genotoxic Possibly carcinogenic	10,13
Sudan Orange G	Chili sauce, turmeric, paprika, cumin, sumac, curry, saffron	No data	11–13
Sudan Red 7B	Chili powder, sausage, turmeric, paprika, cumin, sumac, curry, saffron	Potentially genotoxic Possibly carcinogenic	10,11
Para Red	Turmeric, paprika, cumin, sumac, curry	Potentially genotoxic Possibly carcinogenic	11
Malachite Green	Milk sweets, confectioneries	Genotoxic Potentially carcinogenic	14
Orange II	Sweets, bakery products, fried fish, turmeric powder	LD_{50} (rat) 10,000 mg kg^{-1} Possibly genotoxic Possibly carcinogenic	14
Metanil Yellow	Sweets, bakery products, fried fish, turmeric powder	Potentially genotoxic Possibly carcinogenic	14

[a]LD_{50} is the median lethal dose.

Table 2: Characteristic literature extraction procedures for rhodamine B in real food samples

Extraction Procedure	Ref
Sample aliquots of 2 g were sonicated and vortexed for 15 min in 1:1 ethyl acetate : cyclohexane. They were then centrifuged at 4000 rpm for 5 min.	35
Samples of 25 mg were incubated in 500 µL of acetonitrile at 70 °C for 2 hr.	15
Sample aliquots of 1 g were sonicated in 10 mL of methanol and then centrifuged at 6800 rpm for 5 min.	32
Homogenized samples of 5 g were shaken in 20 mL of 1:2 0.1 M HCl : Ethanol for 1 min. Then, 20 mL of ethyl acetate was added and shaken for 1 min more. Solutions were centrifuged at 3000 rpm for 1 min. Residual solids were extracted two more times. The ethyl acetate layer was separated and 1 mL of 2.5 M NaOH was added, then 50 mL of saturated NaCl solution. The aqueous layer was removed after shaking and 40 mL of hexane and 20 mL of 0.1 M HCl was added. The aqueous later was removed and diluted with water to 100 mL	30
Samples were ground in 2% ammonia in 70% alcohol and left to extract overnight. Samples were centrifuged and the resulting supernatants preconcentrated by evaporation.	14
Oil sample was directly diluted to 10 ppm in methanol	33

Table 3: Characteristic TLC conditions for the analysis of rhodamine B in real food samples

Mobile Phase	Spotting Volume	Ref
ethyl acetate : methanol (8:2)	25 µL	15
2-butanone : methanol : 5% wt/wt Na_2SO_4 (1:1:1)	5 – 20 µL	30
cyclohexane : ethyl acetate (6:1)	-	33

3. METHODOLOGY

3.1. Instrumental Setup

For this method, the instrumental setup shown in Figure 3 was assembled. The setup consists of a lab-made FOP coupled to two spectrofluorometers. The first is an example of a typical commercial spectrofluorometer, the FluoroMax-3 (Horiba Ltd.), and the second is a lab-made instrument combining a Radiant 335 tunable laser system (Opotek Inc.) excitation source with a Shamrock 303i-B spectrograph (Andor Technology Ltd.) equipped with a 1200 grooves mm^{-1} holographic diffraction grating blazed at 500 nm, and an iStar DH320T-18U-63 (Andor Technology Ltd.) intensified charge coupled device (ICCD).[41] The FOP coupled to the commercial spectrofluorometer is an "eight-around-two" bifurcated probe consisting of two bundles of optical fiber — an excitation bundle of two optical fibers in a linear arrangement, and an emission bundle of eight optical fibers in a rectangular arrangement. These bundles converge at the end of the probe, where they are arranged so that the eight emission fibers surround the two excitation fibers. The FOP coupled to the pulsed laser system is a "six-around-one" probe, which is constructed in and operates in a similar manner to the "eight-around-two probe". Both probe designs are illustrated in Figure 4. The excitation bundles of the FOPs deliver monochromatic light from the excitation monochromator of the commercial spectrofluorometer or the output of the pulsed laser, casting a cone of light onto the TLC spot, causing photoluminescence of the analyte. The emission bundle of the FOP guides the photoluminescent radiation emitted by the TLC spot to the emission monochromator of the spectrofluorometer or the spectrograph of the laser system, and subsequently to the detection units. The fiber bundles are incased in a rigid copper housing, which allows the probe to be secured in a fixed position with a burette clamp. In the laser system, liquid

solutions measurements are also taken using the FOP. This is achieved through the addition of a screw cap fixed near the end of the FOP, to which can be attached a vial at a reproducible distance and orientation. The liquid solution is deposited in the vial and attached to the FOP for measurement in an identical manner to the TLC plates. With this system, excitation and emission spectra, photoluminescence lifetimes, and higher-order data formats are recorded. Photoluminescence lifetimes are measured with the pulsed laser, which provides a time-resolved decay plot, from which the lifetime (τ) is determined by interpolating the time where intensity equals the initial intensity divided by Euler's number.

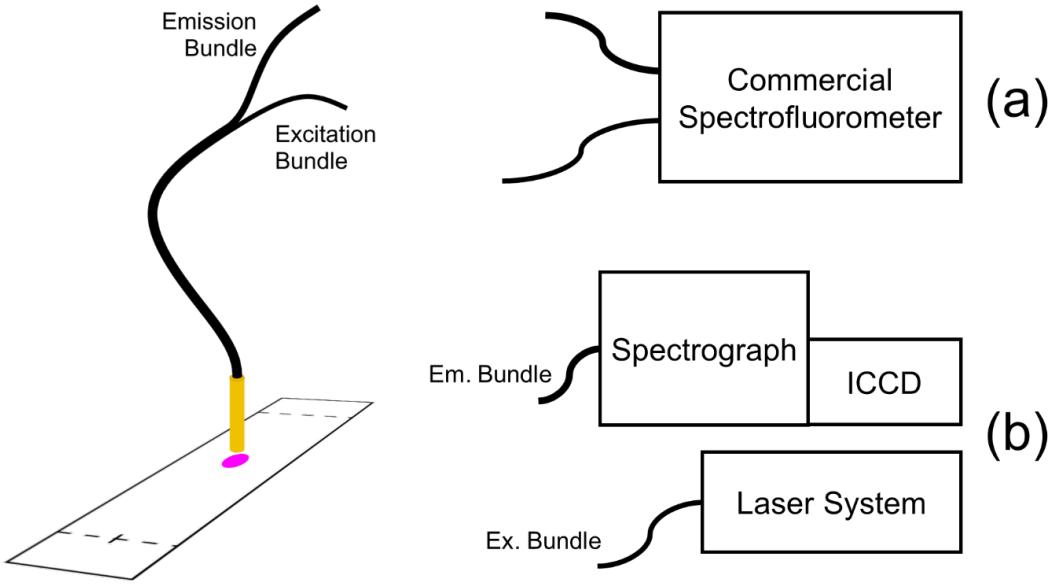

Figure 3: Instrumental schematic used in this work

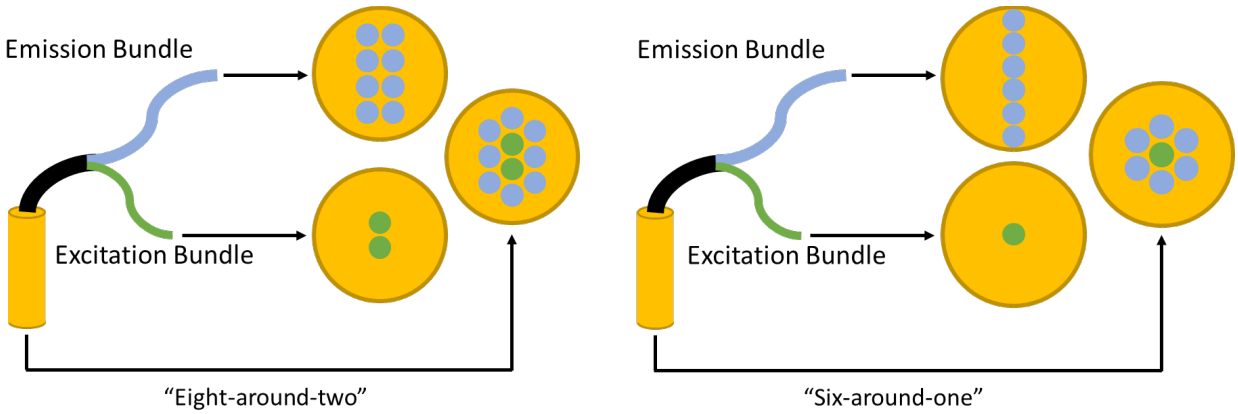

Figure 4: Cross sections of "eight-around-two" and "six-around-one" FOP bundles

3.2. Data Collection and Instrumental Parameters

Initially, full excitation and emission spectra of RhB were collected in triplicate with the commercial spectrofluorometer in liquid solution. Measurements were taken with 500 µL aliquots of sample in a quartz cuvette. Maximum excitation and emission wavelengths were found, and an offset of 30 nm was applied in the negative direction for excitation wavelength, and in the positive direction for emission wavelength, to allow for complete overlapping spectral collection without the contribution of scattering. Full spectra were then taken on RhB immobilized on the TLC plate in an identical manner, using 10 µL of sample. Initially, this was done without chromatographic development, in order to determine optimal acquisition parameters. Acquisition settings for complete spectra are found in Table 4. Collection ranges were selected to eliminate Rayleigh scattering and second order emission, and bandpass was optimized experimentally.

Measurements from the TLC plate were taken by visually centering the FOP above the area of interest. In initial measurements, this was the spotted location, and after chromatographic development, the probe was centered at the expected location of the RhB spot determined by the

R_f and the lane position. After centering, the probe and plate were shrouded as best possible with a cardboard box and black-out cloth to reduce interference from ambient light.

Table 4: Full-spectrum acquisition parameters

	Excitation Spectra		**Emission Spectra**	
Parameter	Liquid Solution	TLC Plate	Liquid Solution	TLC Plate
λ_{ex} / λ_{em}[a]	608 nm	598 nm	525 nm	520 nm
Collection Range	316 – 596 nm	311 – 586 nm	537 – 700 nm	532 – 700 nm
Bandpass	1.50 nm	1.50 nm	1.50 nm	1.50 nm
Increment	1.00 nm	1.00 nm	1.00 nm	1.00 nm
Integration Time	100 ms	100 ms	100 ms	100 ms

[a]Excitation and emission wavelength maxima

For calibration curve measurements with the commercial spectrofluorometer, acquisition settings are found in Table 5. Excitation and emission wavelength maxima were used, and bandpass was optimized experimentally to maximize signal-to-background ratio and avoid scattering and detector saturation.

Table 5: Calibration curve acquisition parameters

Parameter	Liquid Solution	TLC Plate
λ_{ex}[a]	555 nm	550 nm
λ_{em}[b]	578 nm	568 nm
Bandpass	1.50 nm	1.50 nm
Increment	1.00 nm	1.00 nm
Integration Time	100 ms	100 ms

[a]Maximum wavelength of excitation

[b]Maximum wavelength of emission

With the laser system, partial excitation and emission spectra of RhB were taken in triplicate to determine experimental wavelength maxima for the instrument both in liquid solution

and on the TLC plate. Emission spectra were then collected of both a 161 ng mL^{-1} RhB standard, and a blank in triplicate in order to estimate a limit of detection for the laser system. Parameters for emission spectra on the laser are given in Table 7. Lifetime measurements were then taken with the laser system using the stroboscopic optical boxcar method,[46] by collecting WTMs in quintuplicate for both in liquid solution and on the TLC plate. Plots of intensity versus time were extracted at the emission wavelength maxima, exponential fits were applied, and lifetimes were extracted. All measurements were made with an ICCD temperature of -35°C and a gain of 1600 dB. Data collection was performed with lab-made software integrating the instrumental components. WTM acquisition parameters are found in Table 8.

Table 6: Laser-system excitation spectra acquisition parameters

Parameter	Liquid Solution	TLC Plate
λ_{em}[a]	580 nm	570 nm
Excitation Range	480 – 570 nm	535 – 555 nm
Spectrograph Slit Width	20.00 µm	10.00 µm
Integration Time	5.0000 ms	5.0000 ms
Accumulations	50	20
Step	0.5 nm	1.0 nm

[a]Maximum wavelength of emission

Table 7: Laser-system emission spectra acquisition parameters

Parameter	Liquid Solution	TLC Plate
λ_{ex}[a]	550.0 nm	540.0 nm
Emission Range	560 – 600 nm	555 – 590 nm
Spectrograph Slit Width	100.00 µm	10.00 µm
Integration Time	5.0000 ms	5.0000 ms
Accumulations	50	10

[a]Maximum wavelength of excitation

Table 8: WTM acquisition parameters

Parameter	Liquid Solution	TLC Plate
λ_{ex}[a]	550 nm	540 nm
Emission Range	560 – 595 nm	555 – 590 nm
Spectrograph Slit Width	100.00 μm	10.00 μm
Accumulation Integration Time	5.0000 ms	5.0000 ms
Accumulations	50	10
Kinetic Integration Time	250.0 ms	500.0 ms
Kinetic Points	20	22
Gate Delay	113.000 ns	113.000 ns
Gate Width	6.800 ns	11.000 ns
Gate Step	0.340 ns	0.500 ns

[a]Maximum excitation wavelength

Table 9: EEM acquisition parameters

Parameter	TLC Plate
λ_{ex}[a]	250 nm – 600 nm
Emission Range	518 nm – 700 nm
Bandpass	1.50 nm
Excitation Increment	2.00 nm
Emission Increment	2.00 nm
Integration Time	100 ms

[a]Maximum excitation wavelength

Table 10: Synchronous scan acquisition parameters

Parameter	TLC Plate
$\Delta\lambda$[a]	12 nm, 8 nm, 4 nm
Emission Range	258 nm – 708 nm
Bandpass	1.00 nm
Increment	1.00 nm
Integration Time	100 ms

[a]Wavelength offset

3.3. Standard Solution Preparation

A stock solution of 104.8 ± 0.2 μg mL^{-1} RhB was prepared from 5.24 mg of rhodamine B hydrochloride salt (~95% purity) (Sigma-Aldrich) in 50.00 mL of HPLC-grade acetonitrile (ACN) (Sigma-Aldrich) using an analytical balance and a volumetric flask. This stock solution was diluted to 350 ng mL^{-1} with a micropipette and volumetric flask, and further standard solutions of lower concentration were prepared through serial dilution with volumetric glassware.

3.4. TLC and Spotting Conditions

For all SS-RTPLS measurements, 20 cm x 20 cm silica gel TLC plates with a polyester backing (Whatman Ltd.) were used as the solid medium. A 25 μL blunt-needle microsyringe (Thermo Fisher Scientific Inc.) was used to spot 10 μL aliquots of sample onto the substrate by drawing sample up to the 15 μL mark, expelling down to the 10 μL mark, wiping the needle to remove excess liquid, lightly placing the tip of the syringe level on the TLC plate, and expelling the solution in a single, smooth motion. Before a sample was spotted, the syringe was acclimated to the sample by washing five times with 20 μL of sample each wash. In between samples, the syringe was washed twenty times with 20 μL of ACN each wash.

For initial measurements without development of the TLC plates, 5 cm x 10 cm sections were cut out of the main plates. Standard solutions of RhB and blank solutions of ACN were spotted on these sections in the manner illustrated in Figure 5, where the spots labeled “S1”, “S2”, and “S3” are sample solutions of a given concentration 1, 2, or 3, and the spots labeled “B” are blanks. This arrangement allows for a full sampling of the TLC plate to ensure uniformity.

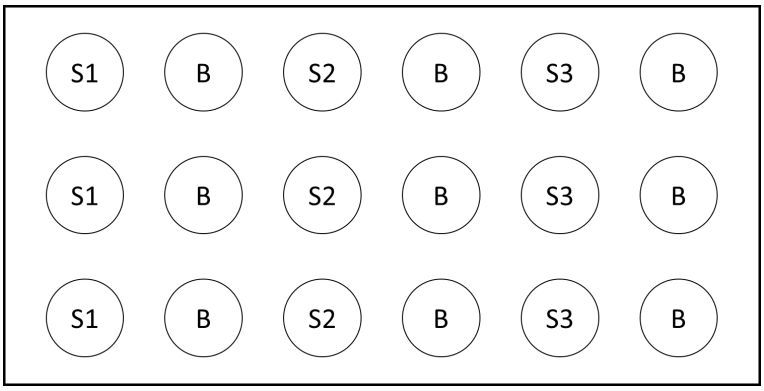

Figure 5: Diagram of the non-developed TLC plate spotting scheme

For measurements with development of the TLC plates, 5 cm x 8.5 cm sections were cut out of the main plates. Standard solutions of RhB and blank solutions of HPLC-grade ACN were spotted on these sections in the manner illustrated in Figure 6, where the spots labeled “S” are sample solutions of a given concentration, and the spots labeled “B” are blanks. Spotting was performed 1.0 cm away from the bottom of the plate. For each concentration measured, a new TLC plate was spotted and developed.

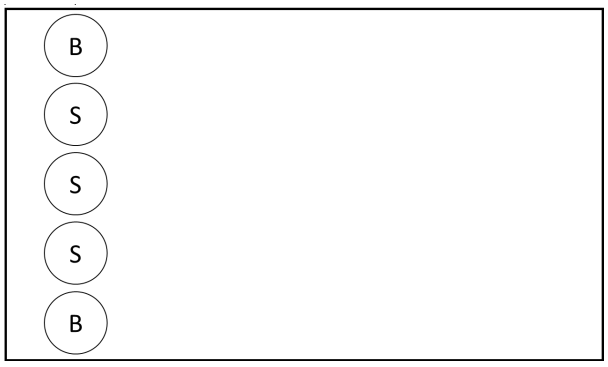

Figure 6: Diagram of the developed TLC plate spotting scheme

TLC development was performed through vertical capillary development in a 250 mL beaker. A section of chromatography paper was used to facilitate saturation mobile phase vapors within the chamber, and a watchglass was used to cover the beaker to maintain equilibrium. The beaker was filled with approximately 15 mL of mobile phase — about 4 mm high. A mobile phase of 8:2 methanol : ethyl acetate was used, prepared with graduated cylinders. HPLC-grade ethyl acetate (EtOAc) and HPLC-grade methanol (MeOH) were obtained from Sigma-Aldrich. TLC plates were developed for 12 minutes at which point they were immediately removed from the beaker, their solvent fronts marked, and allowed to dry at ambient conditions for 10 minutes. R_f values were measured with dial calipers in triplicate for an upper and a lower concentration of RhB.

3.5. Extraction of Food Samples

Chili powder samples were extracted by sonicating 150 mg of powder in 1.000 mL of ACN for 10 minutes at room temperature. Samples were then centrifuged for 5 minutes at 8000 rpm. Four samples were prepared to evaluate the method in the analysis of a real food sample. In the first sample, chili powder was extracted, and no spike was added. The second sample consisted of spiking the chili powder with 15.0 µL of 12.6 ± 0.1 µg mL^{-1} RhB in ACN, allowing the sample to dry for an hour, and extracting. In the third sample, 11.3 µL of 12.6 ± 0.1 µg mL^{-1} RhB in ACN was air-dried to a residue in a centrifuge tube. To the residue, 750 µL of chili powder extract was added. In the fourth sample, 15.0 µL of 12.6 ± 0.1 µg mL^{-1} RhB in ACN was added to a centrifuge tube and dried to a residue, at which point 1.000 mL of ACN was added.

4. RESULTS & DISCUSSION

4.1. Spectral Properties of Rhodamine B in Liquid Solution and under SS-RTPLS

When comparing excitation and emission fluorescence spectra of RhB in both liquid solution of ACN, and immobilized on the TLC plate, taken on the commercial spectrofluorometer, several major differences can be seen. As exhibited by Figure 7, the spectral profile of both excitation and emission bands are nearly identical in shape between the liquid solution and TLC plate measurements. However, there is a significant hypsochromic shift in excitation and emission wavelengths when RhB is immobilized on the TLC plate. A possible explanation for this shift is an energy or charge transfer between the RhB fluorophore and the silica gel, where the excited state dipole moment is lower than the ground state dipole moment.[47] Another possible explanation is that the increased stability of the zwitterionic form of RhB under the high-polarity environment of the silica gel, which has slightly low excitation and emission wavelengths.[48] In addition to the blue shift of the spectra, a significantly lower Stokes' shift is seen on the TLC plate. This can be explained by the increased structural rigidity of the matrix and of the fluorophore when bound to the solid substrate, which decreases the rate of non-radiative processes such as vibrational relaxation, moving the absorption and emission bands closer to each other in energy. This causes an increase in overlap between these two bands, which is advantageous for the collection of synchronous spectra, as it provides high intensity at low wavelength offsets, which enhance selective excitation and spectral simplification.[49]

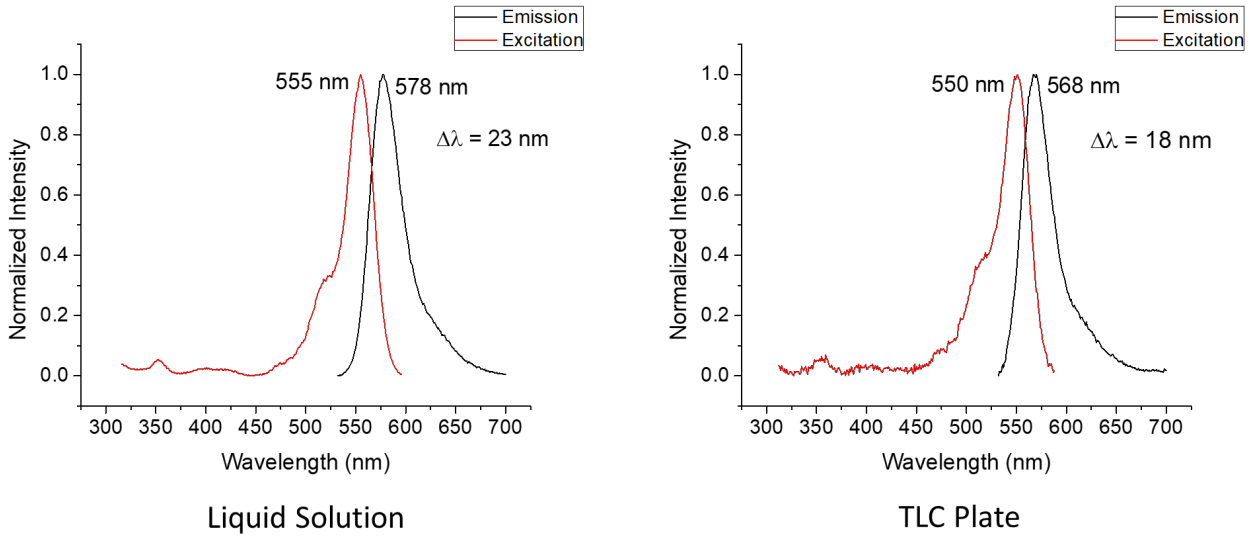

Figure 7: Normalized and blank subtracted excitation and emission spectra of 197 ng mL^{-1} RhB in ACN and 26.9 ng mL^{-1} RhB on a TLC plate recorded on a commercial spectrofluorometer

When evaluating signal-to-background ratio (S/B) for the two methods, the S/B for the conventional liquid solution method is found to be much higher than that of the SS-RTPLS method using the FOP. The low background signal in liquid solution is shown in Figure 8, and while the signal for a given concentration is an order of magnitude higher on the TLC plate, there is unproportionally larger background signal. This is due in part to reflection of excitation light into the emission fiber bundle, which is much greater in the 180° fiber configuration than the 90° spectrofluorometer configuration. This is exhibited by the shoulders seen at the edges of the TLC plate excitation and emission spectra in Figure 8. Additionally, ambient light may contribute to the background signal, as there are likely more leaks in the black-out cloth shroud than in the machined spectrofluorometer sample compartment. Finally, background fluorescence and Raman scattering from the silica gel and polyester backing of the TLC plates may sufficiently contribute to the background signal observed.

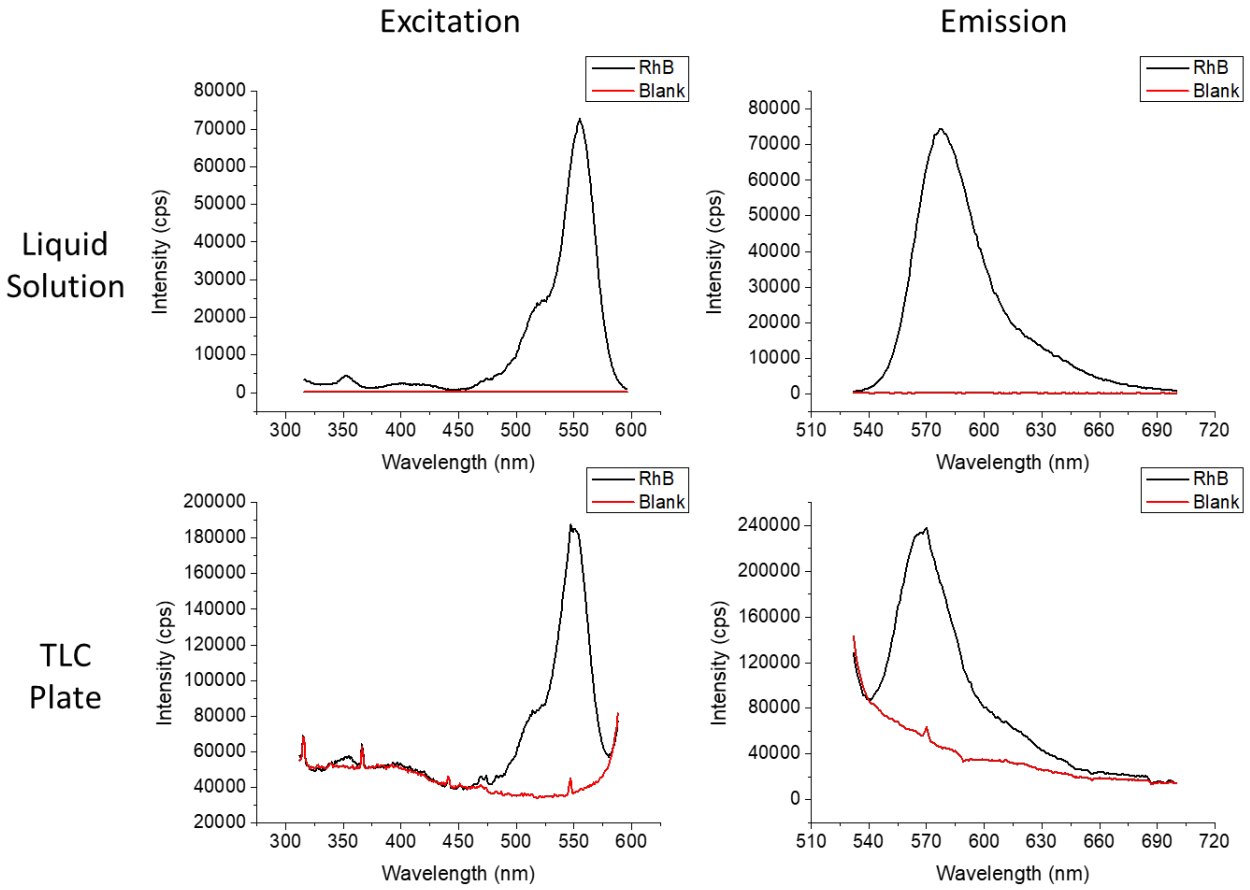

Figure 8: Excitation and emission spectra of 197 ng mL^{-1} RhB in ACN and 161 ng mL^{-1} RhB on a developed TLC plate with blanks of ACN on a TLC plate recorded on a commercial spectrofluorometer

Calibration curves for RhB in liquid ACN solution and immobilized on a TLC plate using identical settings besides excitation and emission wavelength maxima are shown in Figure 9. Both curves show strong linear relationships between concentration or mass of RhB and fluorescence intensity, exhibited by high coefficients of determination. When analytical figures of merit (AFOMs) are compared in Table 11, it is seen that, the LOD of the conventional method in liquid solution is an order of magnitude lower than the SS-RTPLS method using the FOP. However, when these methods are compared by their absolute limits of detection (ALODs), it is seen that they are within the same order of magnitude. Analytical sensitivity (γ) for the SS-RTPLS method

is two orders of magnitude higher than the conventional method on a concentration basis, and three orders of magnitude higher on a mass basis, making it a much more sensitive method. The relative standard deviation (RSD) of the SS-RTPLS method is also lower than the conventional method and is in line with typical fluorescence measurements. The major drawback of the SS-RTPLS method is the narrow linear dynamic range (LDR), which extends less than one order of magnitude, where the convention method spans three orders of magnitude. However, when higher

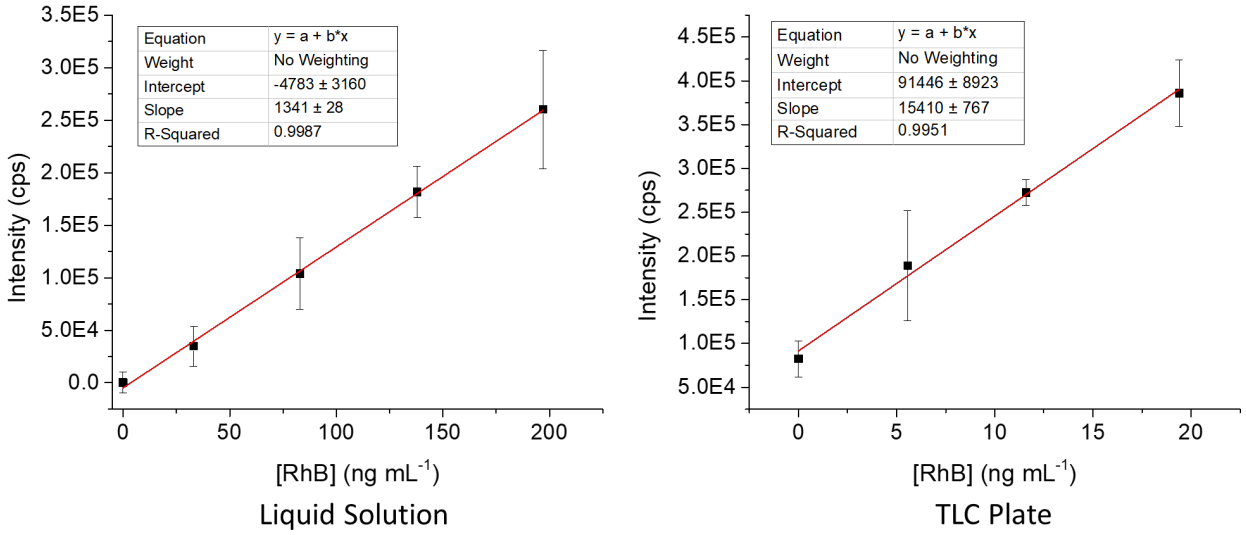

Figure 9: Calibration curves for RhB in ACN and immobilized on a TLC plate

Table 11: Analytical figures of merit for calibration curves of RhB in ACN and on a TLC plate

AFOM	LOD[a] (ng mL^{-1})	ALOD[b] (pg)	LDR[c]	RSD[d]	$\gamma^{d,e}$ (ng^{-1})
Liquid Solution	0.16	81	1.2×10^3	13%	0.1
TLC Plate	4.0	40	4.75	5%	100

[a]Calculated as 3 times the standard deviation of the blank over the slope
[b]Equal to the LOD times the volume of sample used
[c]Equal to the upper limit of linearity divided by the LOD
[d]Taken at the centroid
[e]Calculated as the slope of the calibration curve over the standard deviation of a measurement

concentrations are tested, a second LDR is shown of lower sensitivity from 97 – 350 ng mL^{-1}, extending the range in which quantitative measurements can be taken to two orders of magnitude, up to the limit of linearity of the traditional method on a concentration basis. Both LDRs for the SS-RTPLS method are shown overlaid in Figure 10.

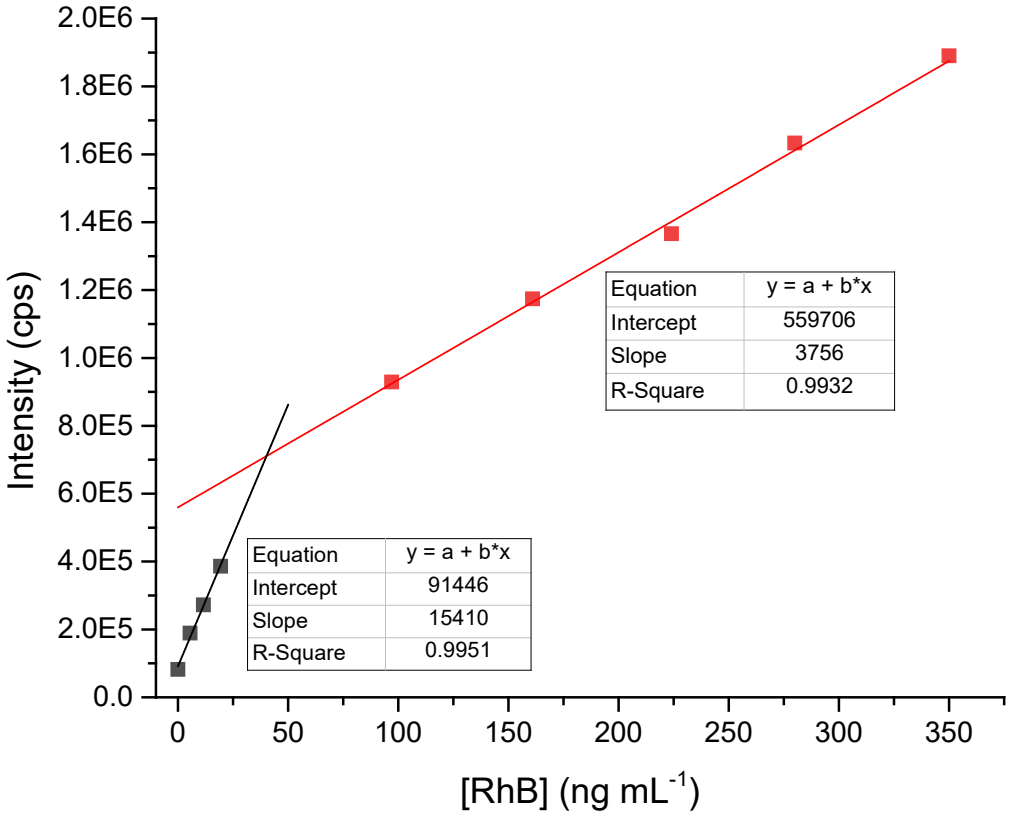

Figure 10: Calibration curve for rhodamine B immobilized on a TLC plate exhibiting two linear dynamic ranges

4.2. Degradation of RhB

During the course of experimentation, it was noticed that over several days in a dark box, the visual fluorescence intensity of RhB decreased over time when immobilized on a TLC plate. This is shown in Figure 11, and suggests a degradation of RhB due to a mechanism other than photobleaching. Because of this, it was determined if solutions of RhB in ACN would degrade over time in the dark under refrigeration. Spectral profiles for three concentrations were compared over a week and are shown in Figure 12. Excitation and emission wavelength maxima stay constant, and additional fluorescence bands do not appear. Additionally, intensity of fluorescence was monitored for the three concentrations and corrected for day-to-day variations with measurements of a DYAG standard (Photon Technology International Inc.). As shown in Table 12, for each concentration, S/B is statistically equivalent for all three days of measurement. Both the spectral consistency and the equivalent intensities indicate stability of refrigerated solutions of RhB in ACN over the concentrations studied.

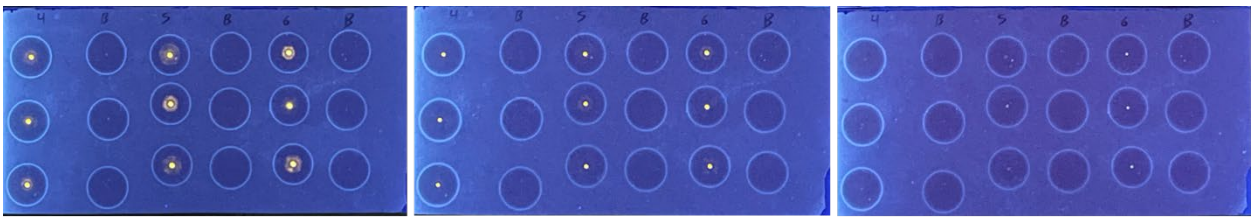

Figure 11: TLC plate with RhB spots of three concentrations visualized under 294 nm light over several days in the dark

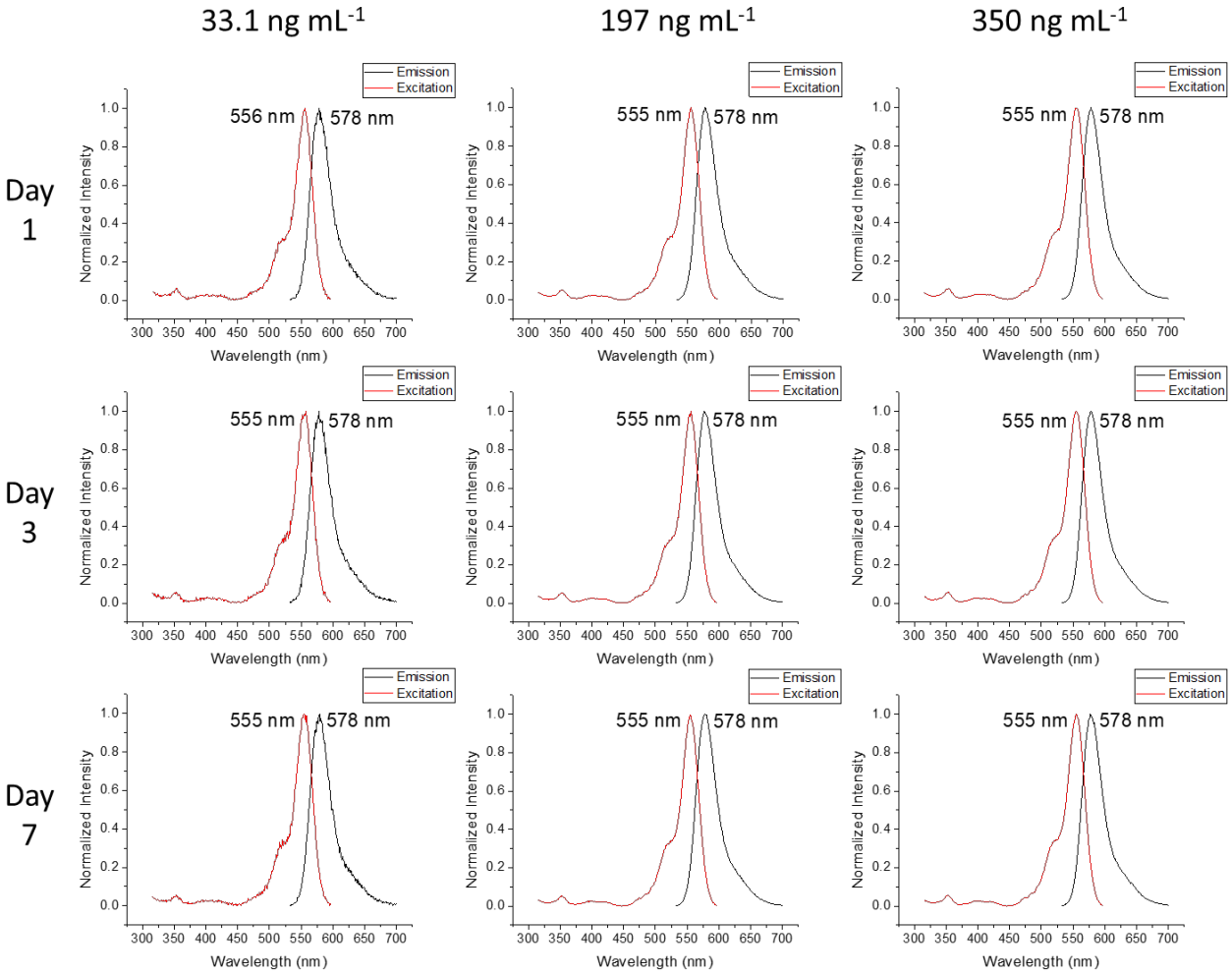

Figure 12: Excitation and emission spectra of three concentrations of RhB in ACN over several days refrigerated in the dark

Table 12: Signal-to-background ratios of three concentrations of RhB in ACN over several days refrigerated in the dark

S/B	33.1 ng mL^{-1}	197 ng mL^{-1}	350 ng mL^{-1}
Day 1	206 ± 88	925 ± 390	2449 ± 327
Day 2	138 ± 70	1855 ± 737	3808 ± 1480
Day 7	350 ± 116	2727 ± 1009	3637 ± 420

4.3. Development of a TLC-SS-RTPLS Calibration Method

The first parameter that requires optimization in any chromatography-based method (column or planar) is mobile phase composition. For the analysis of a single analyte, an R_f value of around 0.5 has been demonstrated to be optimal,[50] and certainly between 0.3 and 0.7. In order to achieve this R_f value, various binary mobile phases of ethyl acetate and methanol were prepared, and the retardation factors a RhB were measured for each. As a highly polar compound, RhB binds strongly to the silica gel substrate of the TLC plate and requires a highly polar mobile phase to cause significant development. Increasing relative methanol concentration was shown to increase polarity index as well as retardation factor, as shown in Table 13. For all future TLC developments in this method, a mobile phase of two parts EtOAc to eight parts MeOH was selected for providing the R_f value nearest to the theoretical optimum.

Table 13: Variation of R_f-values with binary mobile phase mixtures

Mobile Phase	Polarity Index	Retardation Factor (R_f)
8:2 EtOAc-MeOH	4.54	0.067 ± 0.005
6:4 EtOAc-MeOH	4.68	0.29 ± 0.02
4:6 EtOAc-MeOH	4.82	0.404 ± 0.007
2:8 EtOAc-MeOH	4.96	0.449 ± 0.007

The next parameter that was optimized was probe distance. The FOP is ideally positioned such that the cone of light from the excitation fibers projects a spot of light onto the TLC plate that is identical in size to the RhB spot. This results in collection of the entire spot, such that quantitative measurements can be accurately made, while collecting as little background signal from the blank TLC plate as possible. By measuring S/B at several distances of the FOP from the TLC plate, it is

seen in Table 14 that the maximum S/B while maintaining linear response with concentration is observed at 7 mm. The FOP was therefore fixed at this distance for the entire calibration method.

Table 14: Signal-to-background ratios of RhB emission on a TLC plate measured at several probe distances

Probe Distance	7 mm	9 mm	12 mm
S/B	2.52 ± 0.05	1.89 ± 0.09	1.32 ± 0.04

With spectral acquisition settings, mobile phase, and probe distance optimized, a calibration curve was run. As seen in Figure 13, strong linear correlation is observed between fluorescence intensity and concentration of RhB developed on the TLC plate. Excellent AFOMs are demonstrated in Table 15. The LOD is an order of magnitude higher than that of the traditional cuvette method, but the ALOD is in the same order of magnitude and is significantly lower. The LDR spans two orders of magnitude and is comparable to the traditional method. Analytical sensitivity is identical to the traditional method on a concentration basis but is an order of magnitude greater on a mass basis. RSD is higher in the TLC-SS-RTPLS method than the traditional method, however, this is expected due to increased variability in sample placement, and variations introduced from TLC development. Spectral features after TLC development were observed to be identical to those taken on the TLC plate without development.

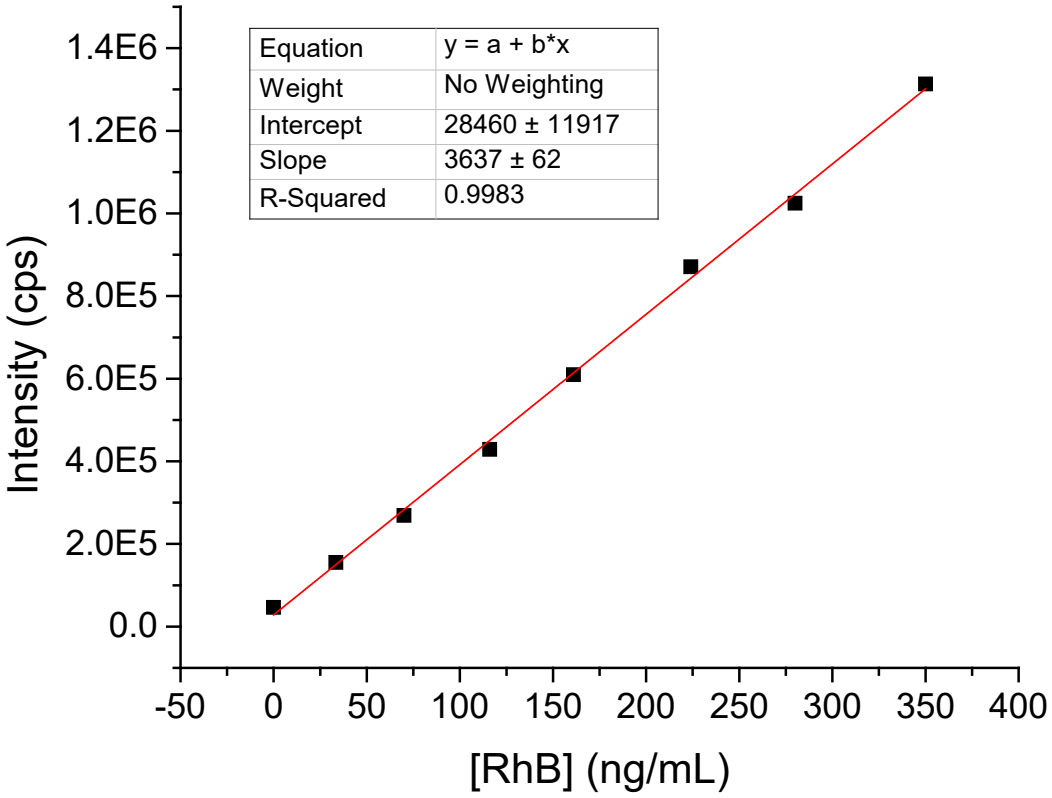

Figure 13: Calibration curve for RhB developed on a TLC plate

Table 15: Analytical figures of merit for RhB calibration curve on a developed TLC plate

AFOM	LOD[a] (ng mL^{-1})	ALOD[b] (pg)	LDR[c]	RSD[d]	$\gamma^{d,e}$ (ng^{-1})
Developed TLC Plate	1.9	19	1.8×10^2	19%	5

[a]Calculated as 3 times the standard deviation of the blank over the slope
[b]Equal to the LOD times the volume of sample used
[c]Equal to the upper limit of linearity divided by the LOD
[d]Taken at the centroid
[e]Calculated as the slope of the calibration curve over the standard deviation of a measurement

4.4. Laser System and Lifetime Data

Excitation and emission spectra of RhB were recorded on the laser system both in ACN solution and immobilized on the TLC plate to determine optimal instrumental parameters for lifetime determination. It can be seen in Figure 14 that excitation and emission wavelength maxima do differ from those on the commercial spectrofluorometer. This is due to differences in the spectral radiance of the xenon lamp and the optical parametric oscillator, as well as differences in spectral efficiency between the monochromator and the spectrograph. The noise evident in the excitation spectra from the laser system is due to variation in laser pulse power and may be compensated for by averaging many spectra or performing many acquisitions. However, photobleaching was observed to be significant on the TLC plate, so total acquisition time was minimized to reduce the effect.

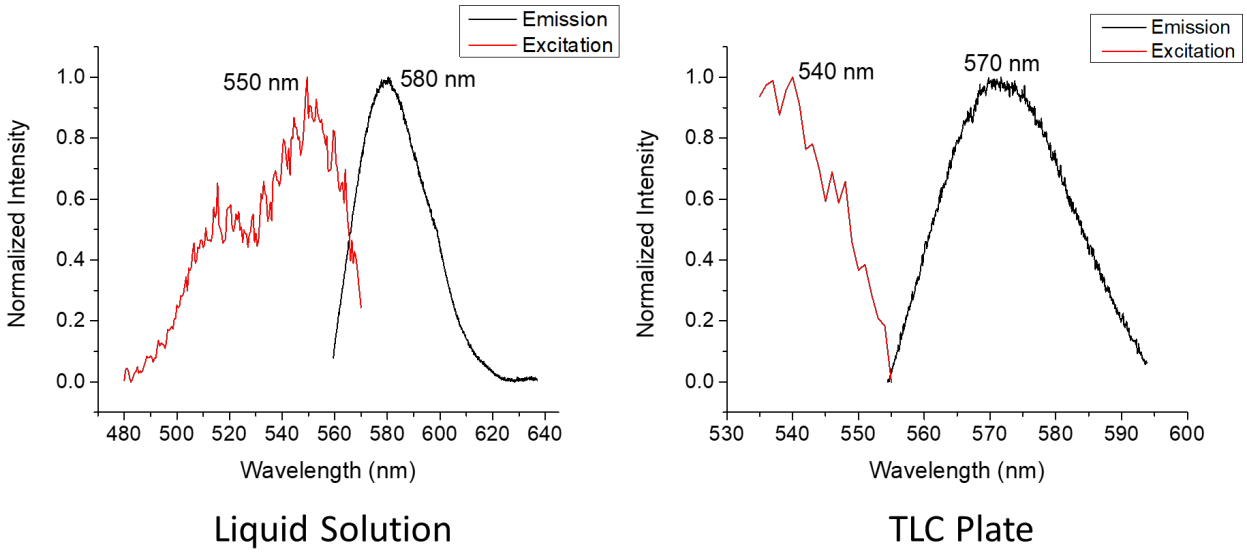

Figure 14: Normalized excitation and emission spectra of 161 ng mL^{-1} RhB in ACN and on a TLC plate recorded on the pulsed laser system

With acquisition settings on the laser system optimized, lifetime measurements of RhB were taken both in liquid solution and on the TLC plate. The fluorescence lifetime decay plots are seen in Figure 15, and exhibit strong fitting with the expected exponential decay function. Fluorescence lifetimes were determined for the plot, and a statistically significant difference in lifetime is observed between the two conditions. The lengthened lifetime on the TLC plate is likely due to the increased structural rigidity of the fluorophore, which decreases the rate of non-radiative decay processes, which in turn increases the lifetime. These lifetime measurements provide another order of data to characterize RhB after chromatographic development, and to separate it from other potential concomitants.

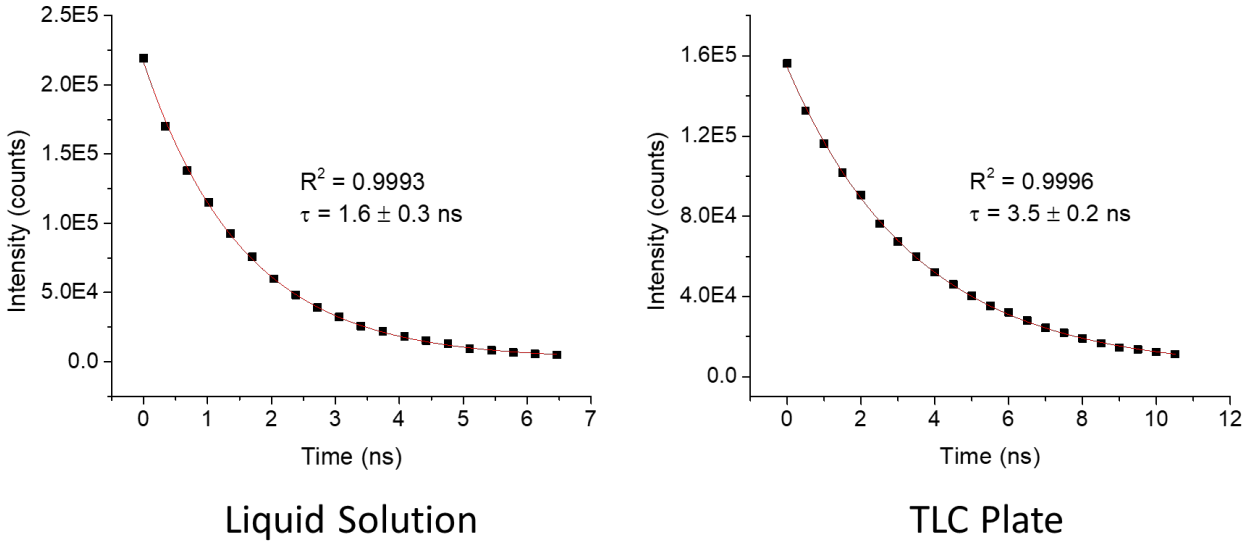

Figure 15: Averages of five fluorescence lifetime decay plots of 161 nm mL^{-1} RhB in ACN and on a TLC plate recorded on the pulsed laser system

4.5. Analysis of Chili Powder

Analysis of a real sample was done thought the calibration curve method with chili powder using the four samples previously described. The standard sample of RhB in pure ACN had a measured concentration of 192 ± 3 ng mL^{-1} RhB, which agrees well with the 190 ng mL^{-1} expected concentration. However, the measured concentration of RhB in the spiked chili powder extract was 117 ± 3 ng mL^{-1}, which is not statistically equivalent to the 190 ng mL^{-1} expected concentration. This indicates significant matrix effects in the measurement of the real chili powder sample reducing the intensity of fluorescence measured from the TLC plate, such as quenching or absorption of excitation light by coeluted concomitants on the TLC plate. However, the measured concentration is still above the LOD of the method, and qualitative data can be taken to confirm the presence of RhB. When a developed TLC plate containing the spiked extract and standard solution is visualized under UV light, shown in Figure 16, fluorescent spots can be seen at the expected R_f value for RhB. When excitation and emission spectra of these spots are analyzed, it can be seen in Figure 17 that spectral profile and excitation and emission wavelength maxima are consistent with those of the standard solution of RhB, suggesting the presence of RhB without significant spectral interference. Lifetime measurements can also be taken on the laser system and show a measured lifetime of 3.8 ± 0.2 ns, which is equivalent to the determined lifetime of pure RhB on a TLC plate. This data supports the unambiguous determination of RhB in the real sample from direct analysis of the TLC plate, at concentrations that are not visibly detectible. To improve the quantitative measurement of this method, it would be best to use the multiple standard additions method of analysis in order to correct for matrix effects in the real sample, however, it may also be possible to mitigate this effect through the use of a more selective extraction procedure, such

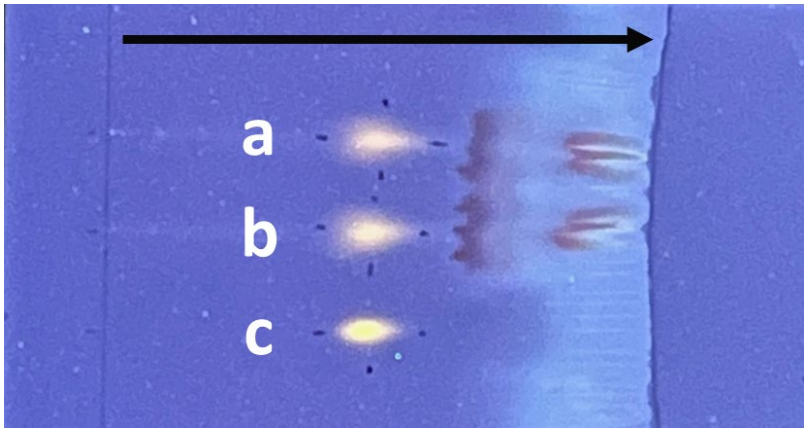

Figure 16: Developed TLC plate visualized under 294 nm light showing (a) spiked chili powder, (b) spiked chili powder extract, and (c) standard RhB solution with the arrow indicating flow direction

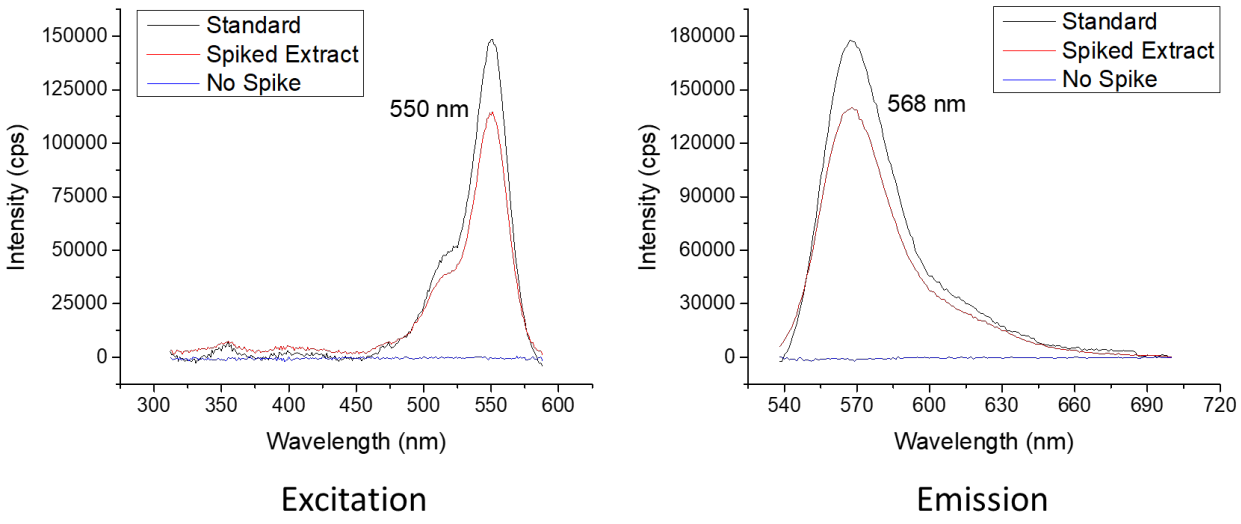

Figure 17: Blank-subtracted excitation and emission spectra in the analysis of chili powder

as SPE, in order to remove concomitants before chromatographic analysis on the TLC plate. As previously mentioned, SPE is already in use for color additive analysis in FDA labs.

Comparing the spiked chili powder extract sample to the sample of extracted spiked chili powder, the extraction efficiency of the method was determined to be 82%. RhB was not detected in the non-spiked chili powder sample.

4.6. Additional and Higher-Order Data Formats

This method and instrumental setup has demonstrated the ability to measure additional data formats directly on the TLC plate, including higher-order data formats. The commercial spectrofluorometer has the ability to collect synchronous scan fluorescence spectra as well as EEMs, which are both shown in Figure 18. As previously mentioned, and as shown in other studies, synchronous scans are useful for spectral simplification, and may allow for the determination of many species that coelute on the TLC plate by using narrow wavelength offsets ($\Delta\lambda$) below 10 nm. It is seen that, for RhB on the TLC plate, a $\Delta\lambda$ = 8 nm provides significant spectral simplification and band narrowing while still showing significant intensity and high S/B. The EEM on the TLC plate shows strong signal and smooth peak profile and would prove useful for non-targeted analysis of fluorophores, as well as spectral deconvolution using chemometrics, leveraging the second-order advantage of this data format.

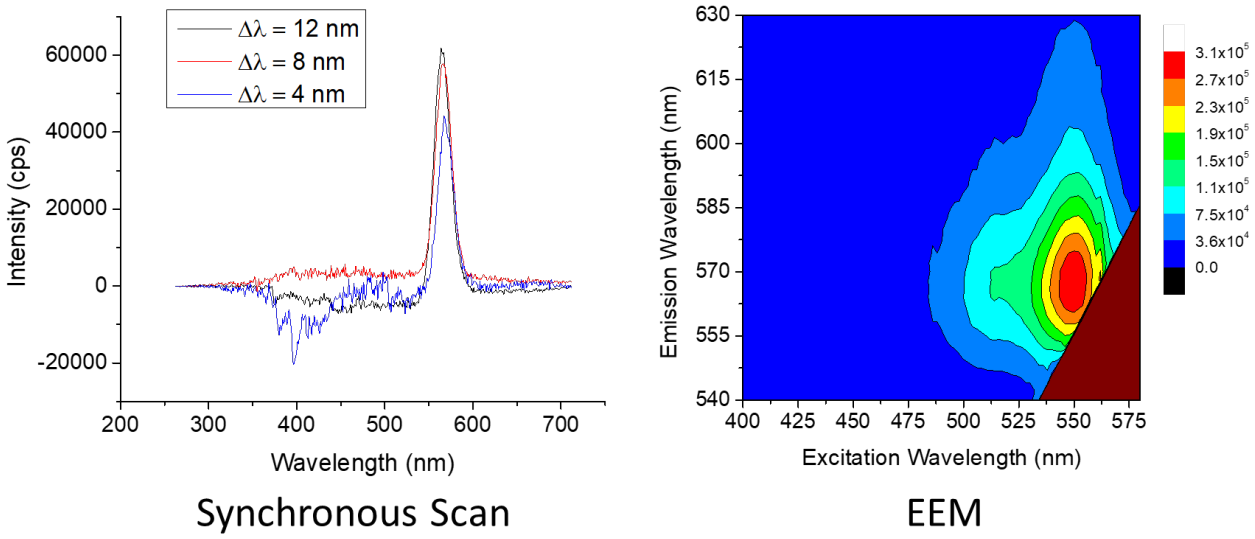

Figure 18: Blank-subtracted synchronous scan spectra and EEM of 161 ng mL^{-1} RhB on a developed TLC plate

Table 16: Properties of synchronous scans at several wavelength offsets

$\Delta\lambda$	λ_{em}[a]	S/B	FWHM[b]
4 nm	565 ± 1	1.3 ± 0.1	19 ± 1
8 nm	565 ± 1	2.2 ± 0.4	19 ± 1
12 nm	564 ± 1	2.6 ± 0.2	20 ± 1

[a]Maximum emission wavelength
[b]Full width at half-maximum

WTMs were successfully collected with the laser system. An additional higher-order data formats, an example WTM of RhB immobilized on a TLC plate is shown in Figure 19. The WTM provides spectral and lifetime information in a single matrix and provides another order of data for chemometric analysis.

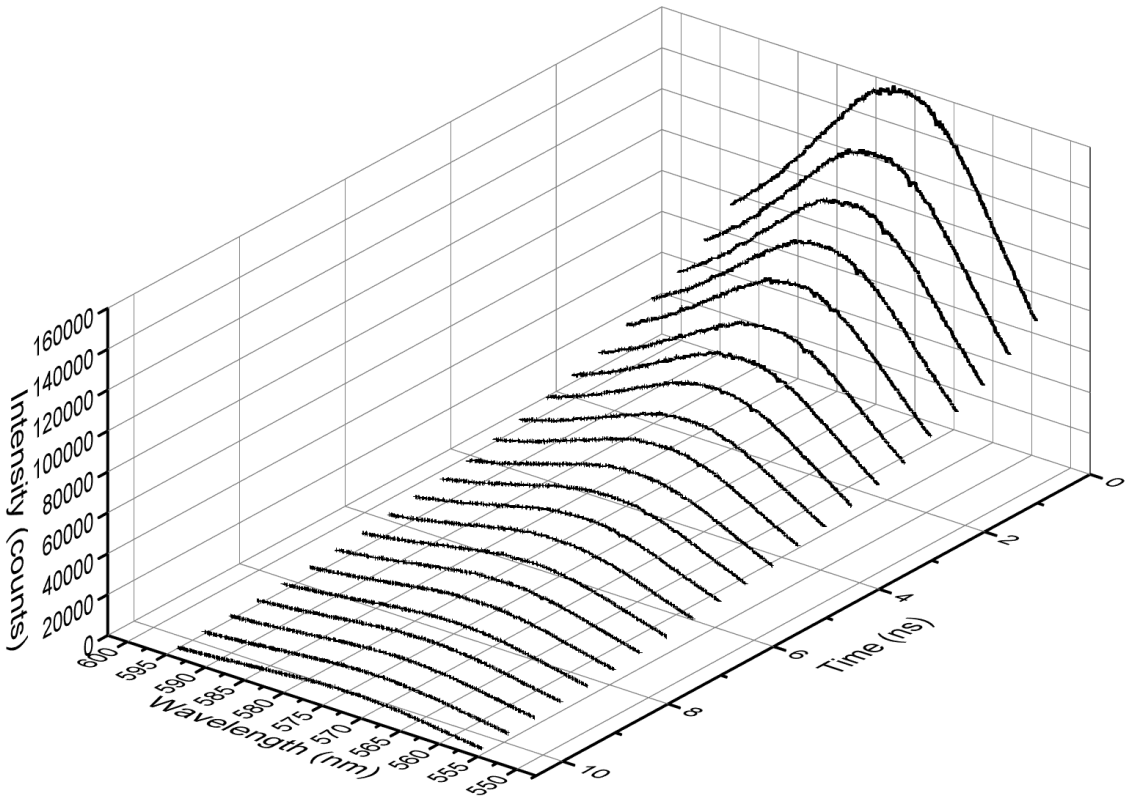

Figure 19: WTM of RhB immobilized on a TLC plate collected on the laser system

4.7. Potential for a Laser-Based Calibration Method

Limits of detection were estimated for RhB in liquid solution and on a developed TLC plate to compare this potential method of analysis to the commercial spectrofluorometer. This was done by analyzing signal-to-noise ratio (S/N), and assuming linearity, where a S/N of 3 is considered to be at the LOD. In liquid solution, the laser system exhibited an LOD of 1.7 ng mL^{-1}, and an ALOD of 170 pg, both of which are higher (poorer) than cuvette measurements in the traditional spectrofluorometer, due to the attenuation and lower collection efficiency of the FOP. However, the developed TLC plate exhibited an LOD of 0.29 ng mL^{-1}, and an ALOD of 2.9 pg, which are the lowest limits of detection reported across all instruments. This is due to the increased radiant power of the laser system compared to the commercial spectrofluorometer, providing increased spectral excitation intensity, and the enhancement of emission through SS-RTPLS. Further optimization of parameters is needed to establish a true lower limit of detection for the laser system on the TLC plate, but these results support the development of a laser-based calibration method with single picogram ALODs.

5. CONCLUSIONS & FUTURE WORK

A screening method for detection of rhodamine B in real food samples was successfully developed based on TLC-SS-RTPLS, where the need for complex liquid chromatography or scrape-dissolution analysis of the TLC plate is eliminated by direct photoluminescence measurement of the TLC spot using a fiber optic probe. The validity of this method was demonstrated with the analysis of chili powder. Compared to traditional chromatographic methods, the developed methodology is substantially more rapid, inexpensive, sustainable, and environmentally friendly for routine monitoring, and provides increased data on which to base positive identification when compared to standard methods of dye analysis. While accurate quantitative analysis of RhB in the real sample was not successful using the calibration curve method, positive identification of RhB was made possible based on retardation factor, photoluminescent intensity, spectral profiles, and photoluminescent lifetimes, all of which were measured directly on the TLC plate. This method exhibits an extremely low absolute limit of detection in the low picogram range using a commercial spectrofluorometer, and the ALOD on the laser system is estimated to be an order of magnitude lower, in the single picogram range. Both the commercial spectrofluorometer and the laser system provide higher-order data formats, of which excitation-emission matrices, and wavelength-time matrices were demonstrated, which may be useful for the analysis of samples with many interfering concomitants through spectral deconvolution using chemometrics.

There are many areas of exploration for future studies and improvements on this method. Expanding the application of this screening method to additional fluorescent dyes other than RhB, where several dyes in a single sample can be separated by TLC and analyzed by SS-RTPLS, is of

interest. Additionally, experiments may be done to improve LODs by reducing S/B through the treatment of TLC plates, as it has been shown with paper that solvent extraction and photobleaching can drastically improve S/B in SS-RTPLS measurements.[51] Additionally, smaller spotting volumes in the nanoliter range have been shown to improve ALODs in laser-induced SS-RTPLS,[52] and may improve ALODs on the developed TLC plate as well. The precision, reproducibility, and throughput of the method may be increased by incorporating some level of automation, as is present in high-performance thin-layer chromatography (HPTLC). Precise mechanical positioning of the TLC plate below the FOP at the desired R_f value would improve reproducibility and lower analysis time. Mechanical control of the probe height would also allow for rapid optimization of distance from the plate, which may differ between multiple dyes. Automated spotting of the plates would also increase precision and decrease total analysis time. If automatization of probe position is implemented, it would be possible to implement imagining techniques, where the FOP is scanned across each lane of the TLC plate, measurements are taken continuously, and a chromatogram is constructed through direct measurement of the plate. This method has been previously implemented using rotating drums and more recently with fluorescent scanners.[53,54] Multiple photoluminescent imaging techniques are present in the literature, however, time-resolved spectroscopy has been limited to a single wavelength.[55] With our instrumental method, time-resolved excitation-emission matrices are possible, which have not been reported on TLC plates in the literature.

6. REFERENCES

(1) 21 U.S.C. § 379 (2007).
(2) 21 C.F.R. § 73 (2022).
(3) *Commission Regulation (EU) No 1129/2011 of 11 November 2011 Amending Annex II to Regulation (EC) No 1333/2008 of the European Parliament and of the Council by Establishing a Union List of Food Additives Text with EEA Relevance*; 2011; Vol. 295. http://data.europa.eu/eli/reg/2011/1129/oj/eng (accessed 2023-03-25).
(4) Dong, M.-Y.; Wu, H.-L.; Long, W.-J.; Wang, T.; Yu, R.-Q. Simultaneous and Rapid Screening and Determination of Twelve Azo Dyes Illegally Added into Food Products by Using Chemometrics-Assisted HPLC-DAD Strategy. *Microchem. J.* **2021**, *171*, 106775. https://doi.org/10.1016/j.microc.2021.106775.
(5) Hu, Z.; Qi, P.; Wang, N.; Zhou, Q.-Q.; Lin, Z.-H.; Chen, Y.-Z.; Mao, X.-W.; Jiang, J.-J.; Li, C. Simultaneous Determination of Multiclass Illegal Dyes with Different Acidic–Basic Properties in Foodstuffs by LC-MS/MS via Polarity Switching Mode. *Food Chem.* **2020**, *309*, 125745. https://doi.org/10.1016/j.foodchem.2019.125745.
(6) Ferrer, C.; Fernández-Alba, A. R.; Ferrer, I. Analysis of Illegal Dyes in Food by LC/TOF-MS. *Int. J. Environ. Anal. Chem.* **2007**, *87* (13–14), 999–1012. https://doi.org/10.1080/03067310701582246.
(7) Qiao, F.; Geng, Y.; He, C.; Wu, Y.; Pan, P. Molecularly Imprinted Microspheres as SPE Sorbent for Selective Extraction of Four Sudan Dyes in Catsup Products. *J. Chromatogr. B* **2011**, *879* (27), 2891–2896. https://doi.org/10.1016/j.jchromb.2011.08.019.
(8) Li, Y.; Wang, Y.; Yang, H.; Gao, Y.; Zhao, H.; Deng, A. Establishment of an Immunoaffinity Chromatography for Simultaneously Selective Extraction of Sudan I, II, III and IV from Food Samples. *J. Chromatogr. A* **2010**, *1217* (50), 7840–7847. https://doi.org/10.1016/j.chroma.2010.10.077.
(9) Yu, W.; Liu, Z.; Li, Q.; Zhang, H.; Yu, Y. Determination of Sudan I–IV in Candy Using Ionic Liquid/Anionic Surfactant Aqueous Two-Phase Extraction Coupled with High-Performance Liquid Chromatography. *Food Chem.* **2015**, *173*, 815–820. https://doi.org/10.1016/j.foodchem.2014.10.091.
(10) Zhang, C.; Li, G.; Zhang, Z. A Hydrazone Covalent Organic Polymer Based Micro-Solid Phase Extraction for Online Analysis of Trace Sudan Dyes in Food Samples. *J. Chromatogr. A* **2015**, *1419*, 1–9. https://doi.org/10.1016/j.chroma.2015.09.059.
(11) Sebaei, A. S.; Youssif, M. I.; Abdel-Maksoud Ghazi, A. Determination of Seven Illegal Dyes in Egyptian Spices by HPLC with Gel Permeation Chromatography Clean Up. *J. Food Compos. Anal.* **2019**, *84*, 103304. https://doi.org/10.1016/j.jfca.2019.103304.
(12) Hemmati, M.; Rajabi, M. Switchable Fatty Acid Based CO2-Effervescence Ameliorated Emulsification Microextraction Prior to High Performance Liquid Chromatography for Efficient Analyses of Toxic Azo Dyes in Foodstuffs. *Food Chem.* **2019**, *286*, 185–190. https://doi.org/10.1016/j.foodchem.2019.01.197.
(13) Bazregar, M.; Rajabi, M.; Yamini, Y.; Arghavani-Beydokhti, S.; Asghari, A. Centrifugeless Dispersive Liquid-Liquid Microextraction Based on Salting-out Phenomenon Followed by High Performance Liquid Chromatography for Determination of Sudan Dyes in Different Species. *Food Chem.* **2018**, *244*, 1–6. https://doi.org/10.1016/j.foodchem.2017.10.006.

(14) Tripathi, M.; Khanna, S. K.; Das, M. Surveillance on Use of Synthetic Colours in Eatables Vis a Vis Prevention of Food Adulteration Act of India. *Food Control* **2007**, *18* (3), 211–219. https://doi.org/10.1016/j.foodcont.2005.09.016.
(15) Bhooma, V.; Nagasathiya, K.; Vairamani, M.; Parani, M. Identification of Synthetic Dyes Magenta III (New Fuchsin) and Rhodamine B as Common Adulterants in Commercial Saffron. *Food Chem.* **2020**, *309*, 125793. https://doi.org/10.1016/j.foodchem.2019.125793.
(16) Wang, M.; Nie, X.; Tian, L.; Hu, J.; Yin, D.; Qiao, H.; Li, T.; Li, Y. Rhodamine B in Spices Determined by a Sensitive UPLC-MS/MS Method. *Food Addit. Contam. Part B* **2019**, *12* (1), 59–64. https://doi.org/10.1080/19393210.2018.1548504.
(17) Authority (EFSA), E. F. S. Opinion of the Scientific Panel on Food Additives, Flavourings, Processing Aids and Materials in Contact with Food (AFC) to Review the Toxicology of a Number of Dyes Illegally Present in Food in the EU. *EFSA J.* **2005**, *3* (9), 263. https://doi.org/10.2903/j.efsa.2005.263.
(18) Jiang, L.-P.; Li, N.; Liu, L.-Q.; Zheng, X.; Du, F.-Y.; Ruan, G.-H. Preparation and Application of Polymerized High Internal Phase Emulsion Monoliths for the Preconcentration and Determination of Malachite Green and Leucomalachite Green in Water Samples. *J. Anal. Test.* **2020**, *4* (4), 264–272. https://doi.org/10.1007/s41664-020-00145-w.
(19) Chen, G.; Miao, S. HPLC Determination and MS Confirmation of Malachite Green, Gentian Violet, and Their Leuco Metabolite Residues in Channel Catfish Muscle. *J. Agric. Food Chem.* **2010**, *58* (12), 7109–7114. https://doi.org/10.1021/jf9043925.
(20) Scalia, S.; Simeoni, S. Assay of Xanthene Dyes in Lipsticks by Inverse Supercritical Fluid Extraction and HPLC. *Chromatographia* **2001**, *53* (9), 490–494. https://doi.org/10.1007/BF02491609.
(21) Borgerding, A. J.; Hites, R. A. Identification and Measurement of Food and Cosmetic Dyes in a Municipal Wastewater Treatment Plant. *Environ. Sci. Technol.* **1994**, *28* (7), 1278–1284. https://doi.org/10.1021/es00056a015.
(22) Feng, C.; Sui, X.; Ankeny, M. A.; Vinueza, N. R. Identification and Quantification of CI Reactive Blue 19 Dye Degradation Product in Soil. *Color. Technol.* **2021**, *137* (3), 251–258. https://doi.org/10.1111/cote.12527.
(23) Adlnasab, L.; Ezoddin, M.; Karimi, M. A.; Hatamikia, N. MCM-41@Cu–Fe–LDH Magnetic Nanoparticles Modified with Cationic Surfactant for Removal of Alizarin Yellow from Water Samples and Its Determination with HPLC. *Res. Chem. Intermed.* **2018**, *44* (5), 3249–3265. https://doi.org/10.1007/s11164-018-3304-5.
(24) Young, M. L. Rapid Identification of Color Additives, Using the C18 Cartridge: Collaborative Study. *J. Assoc. Off. Anal. Chem.* **1988**, *71* (3), 458–461. https://doi.org/10.1093/jaoac/71.3.458.
(25) *AOAC Official Method 988.13*; AOAC: Rockville, MD, 2005.
(26) Yoshioka, N.; Ichihashi, K. Determination of 40 Synthetic Food Colors in Drinks and Candies by High-Performance Liquid Chromatography Using a Short Column with Photodiode Array Detection. *Talanta* **2008**, *74* (5), 1408–1413. https://doi.org/10.1016/j.talanta.2007.09.015.
(27) Chapter 09 - Food and Color Additives. In *Compliance Program Guidance Manual*; Program #7309.006; FDA, 2019.

(28) Mukherjee, S.; Ghati, A.; Paul, G. An Ultraviolet–Visible Spectrophotometric Approach to Establish a Method for Determining the Presence of Rhodamine B in Food Articles. *ACS Food Sci. Technol.* **2021**, *1* (9), 1615–1622. https://doi.org/10.1021/acsfoodscitech.1c00172.
(29) Cheng, Y.-Y.; Tsai, T.-H. A Validated LC–MS/MS Determination Method for the Illegal Food Additive Rhodamine B: Applications of a Pharmacokinetic Study in Rats. *J. Pharm. Biomed. Anal.* **2016**, *125*, 394–399. https://doi.org/10.1016/j.jpba.2016.04.018.
(30) Tatebe, C.; Zhong, X.; Ohtsuki, T.; Kubota, H.; Sato, K.; Akiyama, H. A Simple and Rapid Chromatographic Method to Determine Unauthorized Basic Colorants (Rhodamine B, Auramine O, and Pararosaniline) in Processed Foods. *Food Sci. Nutr.* **2014**, *2* (5), 547–556. https://doi.org/10.1002/fsn3.127.
(31) Alesso, M.; Bondioli, G.; Talío, M. C.; Luconi, M. O.; Fernández, L. P. Micelles Mediated Separation Fluorimetric Methodology for Rhodamine B Determination in Condiments, Snacks and Candies. *Food Chem.* **2012**, *134* (1), 513–517. https://doi.org/10.1016/j.foodchem.2012.02.110.
(32) Fu, D.-S.; Wu, P.-P.; Zhong, X.-D.; Liu, Q.; Luo, H.-D.; Li, Y.-Q. A Simple Synchronous Fluorescence Approach for Rapid and Sensitive Determination of Rhodamine B in Chilli Products. *Food Anal. Methods* **2015**, *8* (1), 189–194. https://doi.org/10.1007/s12161-014-9891-x.
(33) Sha, X.; Han, S.; Fang, G.; Li, N.; Lin, D.; Hasi, W. A Novel Suitable TLC-SERS Assembly Strategy for Detection of Rhodamine B and Sudan I in Chili Oil. *Food Control* **2022**, *138*, 109040. https://doi.org/10.1016/j.foodcont.2022.109040.
(34) Rubio, S.; Gomez-Hens, A.; Valcarcel, M. Analytical Applications of Synchronous Fluorescence Spectroscopy. *Talanta* **1986**, *33* (8), 633–640. https://doi.org/10.1016/0039-9140(86)80149-7.
(35) Huang, Y.; Wang, D.; Liu, W.; Zheng, L.; Wang, Y.; Liu, X.; Fan, M.; Gong, Z. Rapid Screening of Rhodamine B in Food by Hydrogel Solid-Phase Extraction Coupled with Direct Fluorescence Detection. *Food Chem.* **2020**, *316*, 126378. https://doi.org/10.1016/j.foodchem.2020.126378.
(36) Alfarhani, B.; Al-tameemi, M.; Schenone, A. V.; Goicoechea, H. C.; Barbosa, F.; Campiglia, A. D. Room Temperature Fluorescence Spectroscopy of Benzo[a]Pyrene Metabolites on Octadecyl Extraction Membranes. *Microchem. J.* **2016**, *129*, 83–89. https://doi.org/10.1016/j.microc.2016.06.010.
(37) Calimag-Williams, K.; Goicoechea, H. C.; Campiglia, A. D. Room-Temperature Fluorescence Spectroscopy of Monohydroxy Metabolites of Polycyclic Aromatic Hydrocarbons on Octadecyl Extraction Membranes. *Talanta* **2011**, *85* (4), 1805–1811. https://doi.org/10.1016/j.talanta.2011.07.009.
(38) Olivieri, A. C. Analytical Advantages of Multivariate Data Processing. One, Two, Three, Infinity? *Anal. Chem.* **2008**, *80* (15), 5713–5720. https://doi.org/10.1021/ac800692c.
(39) Santana, A.; Comas, A.; Wise, S.; Wilson, W. B.; and; Campiglia, A. D. Instrumental Improvements for the Trace Analysis of Structural Isomers of Polycyclic Aromatic Hydrocarbons with Molecular Mass 302 Da. *Anal. Chim. Acta* **2020**, *1100*, 163–173. https://doi.org/10.1016/j.aca.2019.10.067.
(40) Moore, A. F. T.; Barbosa, F.; Campiglia, A. D. Combining Cryogenic Fiber Optic Probes with Commercial Spectrofluorimeters for the Synchronous Fluorescence Shpol'skii

Spectroscopy of High Molecular Weight Polycyclic Aromatic Hydrocarbons. *Appl. Spectrosc.* **2014**, *68* (1), 14–25. https://doi.org/10.1366/13-07124.
(41) Campiglia, A. D.; Bystol, A. J.; Yu, S. Instrumentation for Multidimensional Luminescence Spectroscopy and Its Application to Low-Temperature Analysis in Shpol'skii Matrixes and Optically Scattering Media. *Anal. Chem.* **2006**, *78* (2), 484–492. https://doi.org/10.1021/ac051332v.
(42) Alfarhani, B.; Al-Tameemi, M.; Goicoechea, H. C.; Barbosa, F.; Campiglia, A. D. Direct Analysis of Benzo[a]Pyrene Metabolites with Strong Overlapping in Both the Spectral and Lifetime Domains. *Microchem. J.* **2018**, *137*, 51–61. https://doi.org/10.1016/j.microc.2017.09.022.
(43) Muñoz de la Peña, A.; Mujumdar, N.; Heider, E. C.; Goicoechea, H. C.; Muñoz de la Peña, D.; Campiglia, A. D. Nondestructive Total Excitation–Emission Fluorescence Microscopy Combined with Multi-Way Chemometric Analysis for Visually Indistinguishable Single Fiber Discrimination. *Anal. Chem.* **2016**, *88* (5), 2967–2975. https://doi.org/10.1021/acs.analchem.6b00264.
(44) Campiglia, A. D.; Rex, M.; Peña, A. M. de la; Goicoechea, H. C. Excitation–Emission Matrix Fluorescence Spectroscopy Combined with MCR-ALS as a Tool for the Forensic Analysis of Similar and Dissimilar Sets of Textile Fiber Extracts. *Anal. Methods* **2016**, *8* (47), 8314–8321. https://doi.org/10.1039/C6AY02757A.
(45) Moore, A. F. T.; Goicoechea, H. C.; Barbosa, F.; Campiglia, A. D. Parallel Factor Analysis of 4.2 K Excitation–Emission Matrices for the Direct Determination of Dibenzopyrene Isomers in Coal-Tar Samples with a Cryogenic Fiber-Optic Probe Coupled to a Commercial Spectrofluorimeter. *Anal. Chem.* **2015**, *87* (10), 5232–5239. https://doi.org/10.1021/acs.analchem.5b00147.
(46) James, D. R.; Siemiarczuk, A.; Ware, W. R. Stroboscopic Optical Boxcar Technique for the Determination of Fluorescence Lifetimes. *Rev. Sci. Instrum.* **1998**, *63* (2), 1710. https://doi.org/10.1063/1.1143328.
(47) Pavlovich, V. S. Solvatochromism and Nonradiative Decay of Intramolecular Charge-Transfer Excited States: Bands-of-Energy Model, Thermodynamics, and Self-Organization. *ChemPhysChem* **2012**, *13* (18), 4081–4093. https://doi.org/10.1002/cphc.201200426.
(48) Hinckley, D. A.; Seybold, P. G.; Borris, D. P. Solvatochromism and Thermochromism of Rhodamine Solutions. *Spectrochim. Acta Part Mol. Spectrosc.* **1986**, *42* (6), 747–754. https://doi.org/10.1016/0584-8539(86)80095-2.
(49) Vo-Dinh, T. Multicomponent Analysis by Synchronous Luminescence Spectrometry. *Anal. Chem.* **1978**, *50* (3), 396–401. https://doi.org/10.1021/ac50025a010.
(50) Guiochon, G.; Bressolle, F.; Siouffi, A. Study of the Performances of Thin Layer Chromatography. IV—Optimization of Experimental Conditions. *J. Chromatogr. Sci.* **1979**, *17* (7), 368–386. https://doi.org/10.1093/chromsci/17.7.368.
(51) Campiglia, A. D.; De Lima, C. G. Room-Temperature Phosphorimetry of Carbaryl in Low-Background Paper. *Anal. Chem.* **1987**, *59* (23), 2822–2827. https://doi.org/10.1021/ac00150a023.
(52) Campiglia, A. D.; Hueber, D. M.; Vo-Dinh, T. Laser-Induced Solid-Surface Room-Temperature Phosphorimetry of Polycyclic Aromatic Hydrocarbons. *Appl. Spectrosc.* **1996**, *50* (2), 252–256.

(53) Connors, W. M.; Boak, W. K. A Procedure for the Direct Reading of Fluorescent Spots on Thin-Layer Chromatography Plates Using the Turner Fluorometer. *J. Chromatogr. A* **1964**, *16*, 243–245. https://doi.org/10.1016/S0021-9673(01)82472-9.
(54) Coran, S. A.; Bartolucci, G.; Bambagiotti-Alberti, M. Selective Determination of Aloin in Different Matrices by HPTLC Densitometry in Fluorescence Mode. *J. Pharm. Biomed. Anal.* **2011**, *54* (2), 422–425. https://doi.org/10.1016/j.jpba.2010.09.019.
(55) Tozar, T.; Boni, M.; Andrei, I. R.; Pascu, M. L.; Staicu, A. High Performance Thin Layer Chromatography-Densitometry Method Based on Picosecond Laser-Induced Fluorescence for the Analysis of Thioridazine and Its Photoproducts. *J. Chromatogr. A* **2021**, *1655*, 462488. https://doi.org/10.1016/j.chroma.2021.462488.